01 Jun 2010

Phase Transitions of the Generalized Contact Process with Two Absorbing States

Man Young Lee

Thomas Vojta
Missouri University of Science and Technology, vojtat@mst.edu

Recommended Citation

M. Y. Lee and T. Vojta, "Phase Transitions of the Generalized Contact Process with Two Absorbing States," *Physical Review E - Statistical, Nonlinear, and Soft Matter Physics*, vol. 81, no. 6, pp. 061128-1-061128-8, American Physical Society (APS), Jun 2010.
The definitive version is available at https://doi.org/10.1103/PhysRevE.81.061128

Phase transitions of the generalized contact process with two absorbing states

Man Young Lee and Thomas Vojta
Department of Physics, Missouri University of Science and Technology, Rolla, Missouri 65409, USA
(Received 22 March 2010; published 21 June 2010)

We investigate the generalized contact process with two absorbing states in one space dimension by means of large-scale Monte Carlo simulations. Treating the creation rate of active sites between inactive domains as an independent parameter leads to a rich phase diagram. In addition to the conventional active and inactive phases we find a parameter region where the simple contact process is inactive, but an *infinitesimal* creation rate at the boundary between inactive domains is sufficient to take the system into the active phase. Thus, the generalized contact process has two different phase transition lines. The point separating them shares some characteristics with a multicritical point. We also study in detail the critical behaviors of these transitions and their universality.

DOI: 10.1103/PhysRevE.81.061128 PACS number(s): 05.70.Ln, 64.60.Ht, 02.50.Ey

I. INTRODUCTION

Many systems in physics, chemistry, and biology are far from thermal equilibrium, even if they are in time-independent steady states. In recent years, continuous phase transitions between different nonequilibrium steady states have attracted lots of attention. Just as in equilibrium, these transitions are characterized by large-scale fluctuations and collective behavior over large distances and long times. Examples can be found, e.g., in surface growth, granular flow, chemical reactions, population dynamics, and even in traffic jams [1–7].

Continuous nonequilibrium phase transitions can be divided into different universality classes according to their critical behavior, and considerable effort has been devoted to categorizing the variety of known transitions. A well-studied type of nonequilibrium phase transitions separates fluctuating (active) steady states from absorbing (inactive) states where fluctuations stop completely. The generic universality class for these so-called absorbing state transitions is directed percolation (DP) [8]. More specifically, it was conjectured by Janssen and Grassberger [9,10] that all absorbing state transitions with a scalar order parameter and short-range interactions belong to this class as long as there are no extra symmetries or conservation laws. While nonequilibrium transitions in the DP universality class are ubiquitous in both theory and computer simulations, experimental verifications were only found rather recently in ferrofluidic spikes [11] and in the transition between two turbulent states in a liquid crystal [12].

Absorbing state transitions in universality classes different from DP can occur in the presence of additional symmetries or conservation laws. Hinrichsen [13] introduced nonequilibrium lattice models with $n \geq 2$ absorbing states. In the case of two symmetric absorbing states ($n=2$), he found the transition to be in a new universality class, the Z_2-symmetric directed percolation class (DP2). If the symmetry between the absorbing states is broken, the critical behavior reverts back to DP. In one dimension, the DP2 universality class coincides [4] with the parity-conserving PC class [14] which is observed, e.g., in the branching-annihilating random walk with an even number of offspring (BARWE) [15].

In this paper, we revisit one of the stochastic lattice models introduced in Ref. [13], the generalized contact process with two absorbing states in one space dimension. Compared to the simple contact process [16], this model contains an additional dynamical process, viz., the creation of active sites at the boundary between domains of different inactive states. By treating the rate for this process as an independent parameter we uncover a rich phase diagram with two different types of phase transitions, separated by a special point that shares many characteristics with a multicritical point. We perform large-scale Monte Carlo simulations of this model to study in detail the critical behavior of these transitions.

Our paper is organized as follows. We introduce the generalized contact process with several absorbing states in Sec. II In Sec. III, we summarize the mean-field theory for this system. Sec. IV is devoted to the results and interpretation of our Monte-Carlo simulations. We conclude in Sec. V

II. GENERALIZED CONTACT PROCESS WITH SEVERAL ABSORBING STATES

The contact process [16] is a paradigmatic model in the DP universality class. It is defined on a d-dimensional hypercubic lattice. Each lattice site $\mathbf{r}$ can be in one of two states, namely, A, the active (infected) state or I, the inactive (healthy) state. Over the course of the time evolution, active sites can infect their nearest neighbors, or they can become inactive spontaneously. More precisely, the contact process is a continuous-time Markov process during which active sites turn inactive at a rate μ, while inactive sites become infected at a rate $\lambda m/(2d)$ where m is the number of active nearest neighbors. The healing rate μ and the infection rate λ are external parameters whose ratio determines the behavior of the system.

If $\mu \gg \lambda$, healing dominates over infection. All infected sites will eventually become inactive, leaving the absorbing state without any active sites the only steady state. Thus, the system is in the inactive phase. In the opposite limit, $\lambda \gg \mu$, the infection survives for infinite times, i.e., there is a steady state with a nonzero density of active sites. This is the active phase. The nonequilibrium phase transition between these

two phases at a critical value of the ratio λ/μ is in the DP universality class.

In 1997, Hinrichsen [13] introduced a generalization of the contact process. Each lattice site can now be in one of $n+1$ states, the active state A or one of the n different inactive states I_k $(k=1\ldots n)$. k is sometimes called the "color" index. The dynamics of the generalized contact process is defined via the following rates for transitions of pairs of nearest-neighbor sites,

$$w(\mathrm{AA} \to \mathrm{AI}_k) = w(\mathrm{AA} \to \mathrm{I}_k\mathrm{A}) = \bar{\mu}/n, \tag{1}$$

$$w(\mathrm{AI}_k \to \mathrm{I}_k\mathrm{I}_k) = w(\mathrm{I}_k\mathrm{A} \to \mathrm{I}_k\mathrm{I}_k) = \mu_k, \tag{2}$$

$$w(\mathrm{AI}_k \to \mathrm{AA}) = w(\mathrm{I}_k\mathrm{A} \to \mathrm{AA}) = \lambda, \tag{3}$$

$$w(\mathrm{I}_k\mathrm{I}_l \to \mathrm{I}_k\mathrm{A}) = w(\mathrm{I}_k\mathrm{I}_l \to \mathrm{AI}_l) = \sigma, \tag{4}$$

with $k,l=1\ldots n$ and $k\neq l$. All other rates vanish. We are mostly interested in the fully symmetric case, $\mu_k \equiv \mu$ for all k. For $n=1$ and $\bar{\mu}=\mu$, the so defined generalized contact process coincides with the simple contact process discussed above. One of the rates $\bar{\mu}$, μ, λ, and σ can be set to unity without loss of generality, thereby fixing the unit of time. We choose $\lambda=1$ in the following. Moreover, to keep the parameter space manageable, we focus on the case $\bar{\mu}=\mu$ in the bulk of the paper. The changes for $\bar{\mu}\neq\mu$ will be briefly discussed in Sec. V

The process [Eq. (4)] prevents inactive domains of different color (different k) to stick together indefinitely. They can separate, leaving active sites in between. Thus, this transition allows the domain walls to move through space. It is important to realize that without the process [Eq. (4)], i.e., for $\sigma=0$, the color of the inactive sites becomes unimportant, and all I_k can be identified. Consequently, for $\sigma=0$, the dynamics of the generalized contact process reduces to that of the simple contact process for all values of n.

Hinrichsen [13] studied the one-dimensional generalized contact process by means of Monte Carlo simulations, focusing on the case $\sigma=\lambda=1$. For $n=2$, he found a nonequilibrium phase transition at a finite value of μ which separates the active and inactive phases. The critical behavior of this transition coincides with that of the PC universality class. For $n\geq 3$, he found the model to be always in the active phase. The Monte Carlo simulations were later confirmed by means of a non-Hermitian density-matrix renormalization group study [17].

Motivated by a seeming discrepancy between these results and simulations that we performed during our study of absorbing state transitions on a percolating lattice [18], we revisit the one-dimensional generalized contact process with two inactive states. In contrast to the earlier works we treat the rate σ of the process [Eq. (4)] as an independent parameter (rather than fixing it at $\sigma=\lambda=1$).

III. MEAN-FIELD THEORY

To get a rough overview over the behavior of the generalized contact process with two inactive states, we first perform a mean-field analysis. Denoting the probabilities for a site to be in state A, I_1, and I_2 with P_A, P_1, and P_2, respectively, the mean-field equations read,

$$dP_A/dt = (1-\mu)P_A - P_A^2 + 2\sigma P_1 P_2, \tag{5}$$

$$dP_1/dt = \mu P_A/2 - P_A P_1 - \sigma P_1 P_2, \tag{6}$$

$$dP_2/dt = \mu P_A/2 - P_A P_2 - \sigma P_1 P_2. \tag{7}$$

Let us begin by discussing the steady states which are given by the fixed points of the mean-field equations. There are two trivial, inactive fixed points $P_1=1$, $P_A=P_2=0$ and $P_2=1$, $P_A=P_1=0$. They exist for all values of the parameters μ and σ and correspond to the two absorbing states. In the case of $\sigma=0$, these fixed points are unstable for $\mu<1$ and stable for $\mu>1$. In contrast, for $\sigma>0$, they are always unstable.

The active fixed point is given by $P_1=P_2$ and fulfills the equation

$$0 = (1-\mu)P_A - P_A^2 + \sigma(1-P_A)^2/2. \tag{8}$$

For $\sigma=0$, this equation reduces to the well-known mean-field equation of the simple contact process, $0=(1-\mu)P_A-P_A^2$ with the solution $P_A=1-\mu$ for $\mu<1$. Thus, for $\sigma=0$, the nonequilibrium phase transition of the generalized contact process occurs at $\mu=\mu_c^{cp}=1$. This means, it coincides with the transition of the simple contact process, in agreement with the general arguments given in Sec. II In the general case, $\sigma\neq 0$, the steady state density of active sites, P_A, is given by the positive solution of

$$P_A = \frac{1}{2-\sigma}(1-\mu-\sigma \pm \sqrt{\mu^2 - 2\mu + 1 + 2\mu\sigma}). \tag{9}$$

We are particularly interested in the behavior of P_A for small σ. As long as $\mu<\mu_c^{cp}=1$ (i.e., in the active phase of the simple contact process), a small, nonzero σ only provides a subleading correction to P_A. At $\mu=\mu_c^{cp}=1$, the density of active sites vanishes as $P_A\sim\sqrt{\sigma}$ with $\sigma\to 0$. Finally, for $\mu>\mu_c^{cp}=1$, the density of active sites vanishes as $P_A\sim\sigma/(\mu-1)$.

We thus conclude that within mean-field theory, the generalized contact process with two inactive states is in the active phase for any nonzero σ. This agrees with older mean-field results but disagrees with more sophisticated methods which predict a nonequilibrium transition at a finite value of μ [13,17]. The mean-field dynamics can be worked out in a similar fashion. We find that the approach to the stationary state is exponential in time anywhere in parameter space except for the critical point of the simple contact process at $\mu=1$, $\sigma=0$. However, it is known that mean-field theory does not reflect the correct long-time dynamics of the generalized contact process which is of power-law type [13]. Therefore, we do not analyze the mean-field dynamics in detail.

IV. MONTE CARLO SIMULATIONS

A. Method and overview

We now turn to the main part of the paper, viz., large-scale Monte Carlo simulations of the one-dimensional gen-

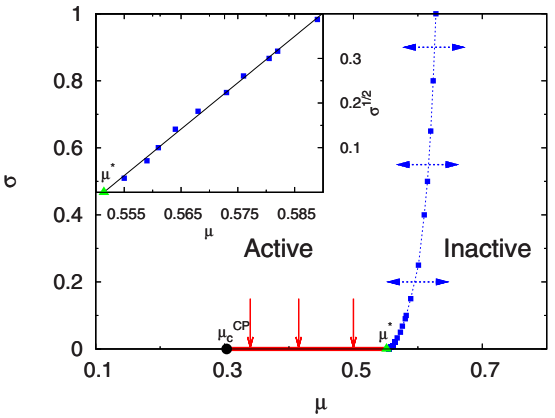

FIG. 1. (Color online) Phase diagram of the 1D generalized contact process as function of the healing rate μ and the boundary rate σ. A line of DP2 (PC) transitions (blue dashed line) separates the active and inactive phases. For $\sigma \to 0$, this line does not terminate in the simple contact process critical point at $\mu_c^{cp} \approx 0.30325$ and but at $\mu^* \approx 0.552$. For $\mu_c^{cp} < \mu < \mu^*$, the system is inactive at $\sigma = 0$ (thick solid red line), but an infinitesimal σ takes it to the active phase. Inset: close to the end point at μ^*, the phase boundary behaves roughly as $\sigma_c \sim (\mu - \mu^*)^2$.

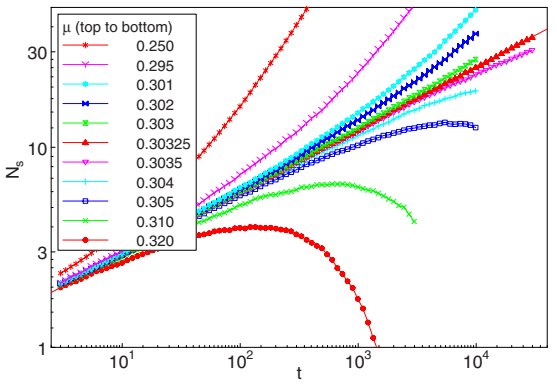

FIG. 2. (Color online) Spreading simulations at $\sigma = 0$: Number N_s of active sites as a function of time t. The solid line for $\mu = 0.30325$ represents a fit to $N_s \sim t^{\Theta_{cp}}$ yielding $\Theta_{cp} = 0.315(5)$. The data are averages over 25 000 runs.

eralized contact process with two inactive states. We perform two different types of calculations: (i) decay runs and (ii) spreading runs. Decay runs start from a completely active lattice; we monitor the time evolution of the density $\rho(t)$ of active sites as well as the densities $\rho_1(t)$ and $\rho_2(t)$ of sites in inactive states I_1 and I_2, respectively. Spreading simulations start from a single active (seed) site embedded in a system of sites in state I_1. (From a domain-wall point of view, the spreading runs are therefore in the even parity sector.) Here we measure the survival probability $P_s(t)$, the number of sites in the active cloud $N_s(t)$ and the mean-square radius of this cloud, $R^2(t)$.

In each case, the simulation proceeds as a sequence of events. In each event, a pair of nearest-neighbor sites is randomly selected from the active region. For the spreading simulations, the active region initially consists of the seed site and its neighbors; it is updated in the course of the simulation according to the actual size of the active cluster. For the decay runs, the active region comprises the entire sample. The selected pair than undergoes one of the possible transitions according to Eqs. (1)–(4) with probability τw. Here the time step τ is a constant which we have fixed at 1/2. The time increment associated with the event is τ / N_{pair} where N_{pair} is the number of nearest-neighbor pairs in the active region.

Using this method we studied systems with sizes up to $L = 10^6$ lattice sites and times up to $t_{max} = 10^8$, exploring the parameter space $0 \le \mu \le 1$ and $0 \le \sigma \le 1$. The $\sigma - \mu$ phase diagram resulting from our simulations is displayed in Fig. 1. This phase diagram shows that the crossover from DP critical behavior at $\sigma = 0$ to DP2 (or, equivalently, PC) critical behavior at $\sigma > 0$ occurs in an unusual fashion. The phase boundary $\sigma_c(\mu)$ between the active and inactive phases does not terminate at the critical point of the simple contact process located at $(\mu, \sigma) = (\mu_c^{cp}, 0) \approx (0.30325, 0)$. Instead, it ends at the point $(\mu, \sigma) = (\mu^*, 0) \approx (0.552, 0)$. In the parameter range $\mu_c^{cp} < \mu < \mu^*$, the system is inactive at $\sigma = 0$, but an infinitesimally small nonzero σ takes it to the active phase.

Thus, the one-dimensional generalized contact process with two inactive states has two types of phase transitions, (i) the generic transition occurring at $\mu > \mu^*$ and $\sigma = \sigma_c(\mu) > 0$ (marked by the dashed blue line and arrows in Fig. 1) and (ii) the transition occurring for $\mu_c^{cp} < \mu < \mu^*$ as σ approaches zero (solid red line and arrows). We note in passing that our critical healing rate for $\sigma = 1$ is $\mu_c = 0.628(1)$, in agreement with Ref. [13].

In the following subsections we first discuss in detail the simulations that lead to this phase diagram, and then we present results on the critical behavior of both transitions as well as special point $(\mu^*, 0) \approx (0.552, 0)$ that separates them.

B. Establishing the phase diagram

We first performed a number of spreading simulations at $\sigma = 0$ and various μ for maximum times up to 3×10^4. The resulting number $N_s(t)$ of active sites in the cluster is shown in Fig. 2. The figure demonstrates that the transition between the active and inactive phases occurs at $\mu = 0.303\ 25(25)$. A fit of the critical curve to $N_s \sim t^{\Theta_{cp}}$ yields $\Theta_{cp} = 0.315(5)$. As expected from the general arguments in Sec. II, both the critical healing rate and the initial slip exponent Θ_{cp} agree very well with the results of the simple contact process (see, e.g., Ref. [19] for accurate estimates of the DP exponents). Thus, at $\sigma = 0$, the generalized contact process undergoes a transition in the directed percolation universality class at $\mu = \mu_c^{cp} = 0.30\ 325(25)$.

We now turn to nonzero σ. Because the domain boundary process [Eq. (4)] creates extra active sites, it is clear that the phase boundary between the active and inactive phases has to shift to larger healing rates μ with increasing σ. In the simplest crossover scenario, the phase boundary $\sigma_c(\mu)$ would behave as $\sigma_c \sim (\mu - \mu_c^{cp})^{1/\phi}$ where ϕ is a crossover exponent. To test this scenario, we performed spreading simulations for times up to 10^7 at several fixed $\mu > \mu_c^{cp}$ in which we vary σ to locate the transition. Examples of the resulting $N_s(t)$ curves for several σ at $\mu = 0.428$ and $\mu = 0.6$ are shown in Fig. 3. The set of curves for $\mu = 0.6$ [Fig. 3(b)]

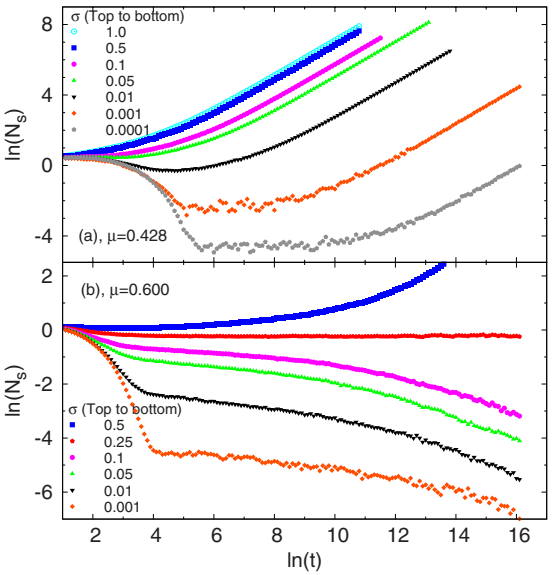

FIG. 3. (Color online) Spreading simulations: Number N_s of active sites as a function of time t for several σ at fixed $\mu=0.428$ (panel a) and $\mu=0.6$ (panel b). The data are averages over 10^3 (at the smallest σ) to 10^5 runs.

behaves as expected: Initially, $N_s(t)$ follows the behavior of the simple contact process at this μ. At later times, the curves with $\sigma \gtrapprox 0.25$ curve upward implying that the system is in the active phase. The curves for $\sigma \lessapprox 0.25$ curve downward, indicating that the system is in the inactive phase. Thus, $\sigma_c(\mu=0.6) \approx 0.25$.

In contrast, the set of curves for $\mu=0.428$ [Fig. 3(a)] behaves very differently. After an initial decay, $N_s(t)$ curves strongly upward for all values of σ down to the smallest value studied, $\sigma=10^{-4}$. This suggests that at $\mu=0.428$, any nonzero σ takes the generalized contact process to the active phase. The phase transition thus occurs at $\sigma=0$.

We determined analogous sets of curves for many different values of the healing rate in the interval $\mu_c^{cp}=0.30325 < \mu < 0.65$. We found that the phase transition to the active phase occurs at $\sigma=0$ for $\mu_c^{cp} < \mu < \mu^*=0.552$, while it occurs at a nonzero σ for healing rates $\mu > \mu^*$. This establishes the phase diagram shown in Fig. 1. The phase boundary thus does *not* follow the simple crossover scenario outlined above. In the following subsections, we analyze in detail the critical behavior of the different nonequilibrium phase transitions.

C. Generic transition

We first consider the generic transition occurring at $\mu > \mu^* \approx 0.552$ and nonzero σ (the blue dashed line in Fig. 1). Figure 4 shows a set of spreading simulations at $\sigma=0.1$ and several μ in the vicinity of the phase boundary. The data indicate a critical point at $\mu \approx 0.582$. We performed analogous simulations for several points on the phase boundary. Figure 5 shows the survival probability P_s and number N_s of active sites as functions of time for all the respective critical points. In log-log representation, the N_s and P_s curves for different σ and μ are perfectly parallel, i.e., they represent

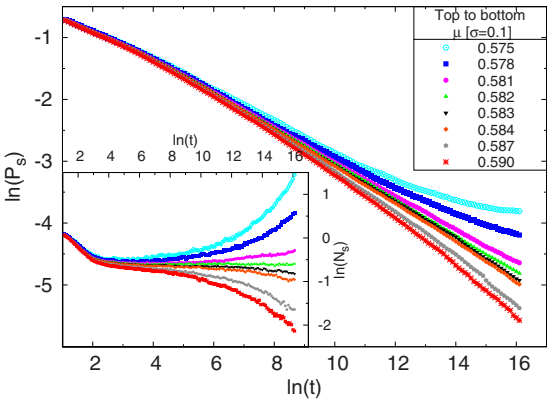

FIG. 4. (Color online) Spreading simulations at $\sigma=0.1$ for several μ close to the phase boundary. Main panel: Number N_s of active sites as a function of time t. Inset: Survival probability P_s as a function of time t. The data are averages over 10^5 runs.

power laws with the same exponent. Fits of the asymptotic long-time behavior to $P_s=B_\sigma t^{-\delta}$ and $N_s=C_\sigma t^{\Theta}$ give estimates of $\delta=0.289(5)$ and $\Theta=0.000(5)$. Moreover, we measured (not shown) the mean-square radius $R^2(t)$ of the active cloud as a function of time. Its long-time behavior follows a universal power law. Fitting to $R^2(t) \sim t^{2/z}$ gives $2/z=1.145(5)$ $[z=1.747(7)]$. Here $z=\nu^{\parallel}/\nu^{\perp}$ is the dynamical exponent, i.e., the ratio between the correlation time exponent $\nu_{\parallel}$ and the correlation length exponent $\nu_{\perp}$.

In addition to the spreading simulations, we also performed density decay simulations for several (μ,σ) points on the phase boundary. Characteristic results are presented in Fig. 6. The figure shows that the density ρ_A of active sites at criticality follows a universal power law, $\rho_A=\bar{B}_\sigma t^{-\alpha}$ at long

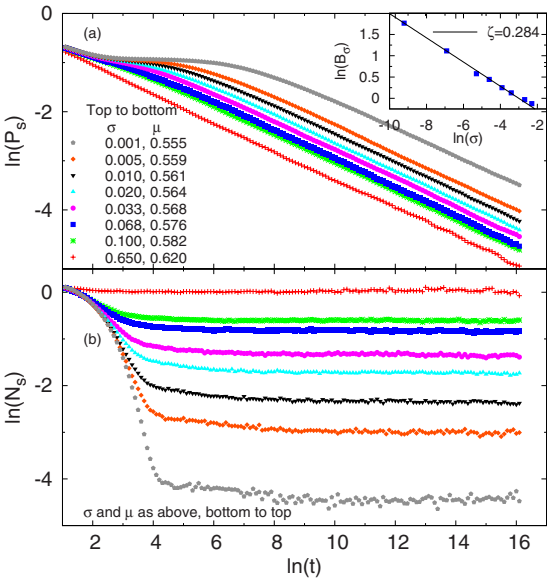

FIG. 5. (Color online) Critical spreading simulations: Survival probability P_s and number of active sites N_s as functions of t for several points (μ,σ) located on the generic phase boundary. The inset shows the prefactor B_σ of the critical power law $P_s=B_\sigma t^{-\delta}$ as a function of σ. The solid line is a fit to $B_\sigma \sim \sigma^{-\zeta}$ which gives $\zeta=0.284$.

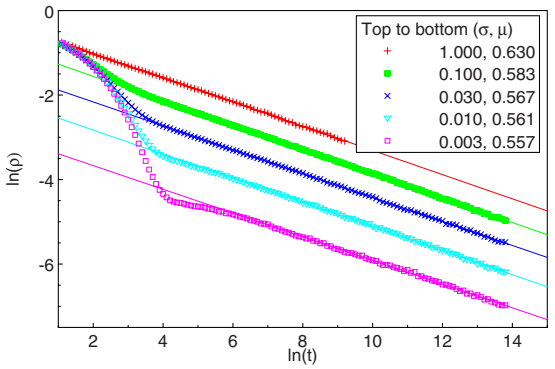

FIG. 6. (Color online) Critical density decay simulations: Density ρ_A of active sites as function of t for several points (μ,σ) on the generic phase boundary. The solid lines are fits to a power law $\rho_A=\bar{B}_\sigma t^{-\alpha}$ giving $\alpha=0.285(5)$. The data represent averages of 400 runs with system size $L=10^4$.

times. The corresponding fits give $\alpha=0.285(5)$ which agrees (within the error bars) with our value of the survival probability exponent δ. We thus conclude that the generic transition of our system is characterized by three independent exponents (for instance $\nu_\perp, z$ and δ) rather than four (as could be expected for a general absorbing state transition [4]). We point out, however, that even though P_s and ρ_A show the same power-law time dependence at criticality, the behavior of the prefactors differs. Specifically, the prefactor $\bar{B}_\sigma$ of the density is increasing with increasing σ while the prefactor B_σ of the survival probability decreases with increasing σ.

All the exponents of the generic transition do not depend on μ or σ, implying that the critical behavior is universal. Moreover, their values are in excellent agreement with the known values of the PC (or DP2) universality class (see, e.g., Refs. [4,5]). We therefore conclude that the critical behavior of the generic transition of generalized contact process with two inactive states is universally in this class.

D. Transition at $\sigma=0$

After discussing the generic transition, we now turn to the line of transitions at $\mu_c^{cp}<\mu<\mu^*$ and $\sigma=0$. To investigate these transitions more closely, we performed both spreading and density decay simulations at fixed μ and several σ-values approaching $\sigma=0$ [as indicated by the solid (red) arrows in the phase diagram, Fig. 1].

Let us start by discussing the density decay simulations. Figure 7 shows the stationary density ρ_{st} of active sites as a function of σ for several values of the healing rate μ. Interestingly, the stationary density depends linearly on σ for all healing rates $\mu_c^{cp}<\mu<\mu^*$, in seeming agreement with mean-field theory. This means $\rho_{st}=B_\mu\sigma^\omega$ with $\omega=1$ and B_μ being a μ-dependent constant. We also analyzed how the prefactor B_μ of the mean-field-like behavior depends on the distance from the simple contact process critical point. As inset (a) of Fig. 7 shows, B_μ diverges as $(\mu-\mu_c^{cp})^{-\kappa}$ with $\kappa=2.3(1)$.

At the critical healing rate μ_c^{cp} of the simple contact process, the stationary density displays a weaker σ-dependence. A fit to a power-law $\rho_{st}\sim\sigma^{\omega_{cp}}$ gives an exponent value of

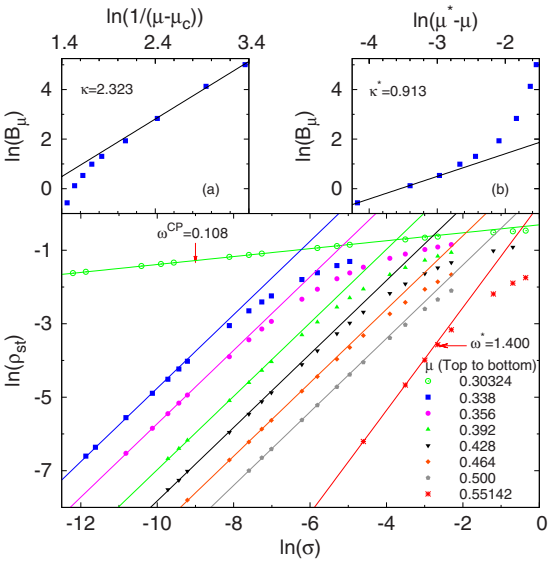

FIG. 7. (Color online) Density decay simulations. Main panel: stationary density ρ_{st} as a function of the boundary rate σ for various healing rates μ. For $\mu_c^{cp}<\mu<\mu^*$, the solid lines are fits of the low-σ behavior to $\rho_{st}=B_\mu\sigma$. At the simple contact process critical point, $\mu=\mu_c^{cp}=0.303\,24$, and at the end point, $\mu=\mu^*=0.552$, we fit to power-laws $\rho_{st}\sim\sigma^\omega$ which gives exponents of $\omega_{cp}=0.108(2)$ and $\omega^*=1.4(1)$. The data are averages over 50 to 200 runs with system sizes $L=2000$ to 5000. Inset a: prefactor B_μ of the linear σ dependence as a function of $\mu-\mu_c^{cp}$. A fit to a power law gives $B_\mu\sim(\mu-\mu_c^{cp})^{-\kappa}$ with $\kappa=2.32(10)$. Inset b: prefactor B_μ as a function of $\mu^*-\mu$. A fit to a power law gives $B_\mu\sim(\mu^*-\mu)^{\kappa^*}$ with $\kappa^*=0.91$.

$\omega_{cp}=0.108(2)$. In contrast, at the end point at healing rate μ^*, the corresponding exponent $\omega^*=1.4(1)$ is larger than 1.

These results of the density decay simulations must be contrasted with those of the spreading simulations. Figure 8 shows the time dependence of the survival probability P_s for $\mu=0.4$ and several σ. At early times, all curves follow the $\sigma=0$ data due to the small values of the rate of the boundary activation process [Eq. (4)]. (Note that the $\sigma=0$ curve does *not* reproduce the survival probability of the simple contact process. This is because in our generalized contact process, a

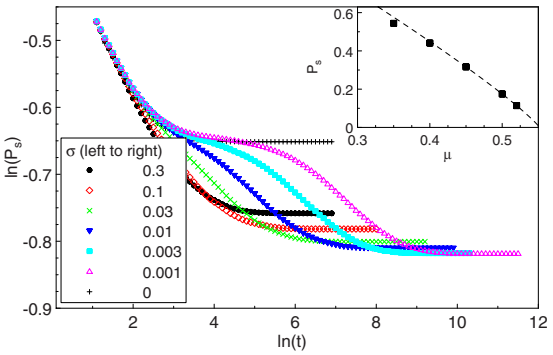

FIG. 8. (Color online) Spreading simulations: Survival probability P_s as a function of time t at $\mu=0.4$ for various values of the boundary rate σ. The data are averages over 100 000 runs. Inset: Low-σ limit of the stationary P_s as a function of μ. The dashed line is a fit to $P_s\sim(\mu^*-\mu)^\beta$ with $\mu^*=0.552$ and $\beta=0.87(5)$ in agreement with the PC universality class (see, e.g., Refs. [4,5]).

sample is surviving as long as not every site is in state I_1 even if there are no active sites.) In the long-time limit, the P_s curves approach nonzero constants, as expected in an active phase. However, in contrast to the stationary density ρ_{st} (Fig. 7), the stationary value of P_s does not go to zero with vanishing boundary rate σ. Instead, it approaches a σ-independent constant. We performed similar sets of simulations at other values of μ in the range $\mu_c^{cp}<\mu<\mu^*$, with analogous results. We therefore conclude that—somewhat surprisingly—the survival probability and the stationary density of active sites display qualitatively different behavior at the $\sigma=0$ phase transition.

We now show that the properties of these quantities can be understood within a simple domain-wall theory. The relevant long-time degrees of freedom at $\mu>\mu_c^{cp}$ and $\sigma\ll 1$ are the domain walls between I_1 and I_2 domains. These domains are formed during the early time evolution when the system follows the simple contact process dynamical rules [Eqs. (1)–(3)]. At late times, the domain walls can hop, they can branch (one wall branching into three), and they can annihilate (two walls vanish if the meet on the same bond between two sites). This means, the domain-wall dynamics follows the branching-annihilating random walk with two offspring (BARW2).

In our case, the BARW2 dynamics is controlled by two rates, the domain-wall hopping rate Γ and the branching rate Ω (annihilation occurs with certainty if two walls meet). These two rates depend on the underlying generalized contact process dynamics. In the limit $\sigma\ll 1$ they are both linear in the boundary rate, $\Gamma=\sigma F_\Gamma(\mu)$, $\Omega=\sigma F_\Omega(\mu)$ because a single boundary activation event is sufficient to start a domain-wall hop or branching (F_Γ and F_Ω are nontrivial functions of μ). Because both rates are linear in σ, their ratio is σ-independent, thus the steady state of the domain walls does not depend on σ in the limit $\sigma\ll 1$. This explains why the survival probability P_s of the generalized contact process saturates at a nonzero, σ-independent value in Fig. 8. It also explains the σ-dependence of the stationary density ρ_{st} of active sites in the following way: For $\sigma\ll 1$ and $\mu>\mu_c^{cp}$, active sites are created mostly at the domain walls at rate σ. Consequently, their stationary density is proportional to both σ and the stationary domain-wall density ρ_{dw}, i.e., $\rho_{st}\sim\sigma\rho_{dw}$, in agreement with Fig. 7. (The linear σ-dependence of ρ_{st} is thus *not* due to the validity of mean-field theory.)

These results imply that the phase transition line at $\sigma=0$ between μ_c^{cp} and μ^* is *not* a true critical line because there is no (nontrivial) diverging length scale. It only appears critical because the stationary density of active sites vanishes with σ. Note that this is also reflected in the fact that the system is not behaving like a critical system right on the phase transition line $\sigma=0$ (no power-law time dependencies, for instance). Instead, the physics of this transition line is controlled by the BARW2 dynamics of the domain walls with a finite correlation length for all $\mu_c^{cp}<\mu<\mu^*$.

E. Scaling at the contact process critical point $(\mu_c^{cp},0)$

Even though the generalized contact process is not critical at $\sigma=0$ and $\mu>\mu_c^{cp}$, its behavior close to the critical point of the simple contact process can be understood in terms of a phenomenological scaling theory.

Let us assume that the stationary density of active sites close to $(\mu_c^{cp},0)$ fulfills the homogeneity relation

$$\rho_{st}(\Delta\mu,\sigma)=b^{\beta_{cp}/\nu_{cp}^{\perp}}\rho_{st}(\Delta\mu b^{-1/\nu_{cp}^{\perp}},\sigma b^{-y_{cp}}) \tag{10}$$

where $\Delta\mu=\mu-\mu_c^{cp}$ and b denotes an arbitrary scale factor. β_{cp} and $\nu_{cp}^{\perp}$ are the usual order parameter and correlation length exponents and y_{cp} denotes the scale dimension of σ at this critical point. Setting $b=\sigma^{1/y_{cp}}$ then gives rise to the scaling form

$$\rho_{st}(\Delta\mu,\sigma)=\sigma^{\beta_{cp}/(\nu_{cp}^{\perp}y_{cp})}X(\Delta\mu\sigma^{-1/(\nu_{cp}^{\perp}y_{cp})}), \tag{11}$$

where X is a scaling function. At criticality, $\Delta\mu=0$, this leads to $\rho_{st}(0,\sigma)\sim\sigma^{\beta_{cp}/(\nu_{cp}^{\perp}y_{cp})}$ [using $X(0)=$const]. Thus, $\omega_{cp}=\beta_{cp}/(\nu_{cp}^{\perp}y_{cp})$. For $\sigma\to 0$ at nonzero $\Delta\mu$, we need the large-argument limit of the scaling function X. On the active side of the critical point, $\Delta\mu<0$, the scaling function must behave as $X(x)\sim|x|^{\beta_{cp}}$ to reproduce the correct critical behavior of the density, $\rho_{st}\sim|\mu-\mu_c^{cp}|^{\beta_{cp}}$.

More interesting is the behavior on the inactive side of the critical point, i.e., for $\Delta\mu>0$ and $\sigma\to 0$. Here, we assume the scaling function to behave as $X(x)\sim x^{-\kappa}$. In this limit, we thus obtain $\rho_{st}\sim(\Delta\mu)^{-\kappa}\sigma^{\omega}$ (just as observed in Fig. 7) with $\omega=(\beta_{cp}+\kappa)/(\nu_{cp}^{\perp}y_{cp})$. As a result of our scaling theory, the exponents ω, ω_{cp} and κ are not independent, they need to fulfill the relation $\omega_{cp}(\beta_{cp}+\kappa)=\beta_{cp}\omega$. Our numerical values, $\omega=1$, $\omega_{cp}=0.108(2)$ and $\kappa=2.32(10)$ fulfill this relation in very good approximation, indicating that they represent asymptotic exponents and validating the homogeneity relation (10). Using $\beta_{cp}=0.2765$ and $\nu_{cp}^{\perp}=1.097$ [19], the resulting value for the scale dimension y_{cp} of σ at the simple contact process critical point is $y_{cp}=2.34(4)$.

F. End point $(\mu^*,0)$

Finally, we turn to the point $(\mu^*,\sigma)=(0.552,0)$ where the generic phase transition line terminates on the μ axis. At first glance, one might suspect this point to be a multicritical point because it is located at the intersection of two phase transition lines. However, we argued in Sec. IV D (based on the domain-wall theory) that the transition line at $\sigma=0$ and $\mu_c^{cp}<\mu<\mu^*$ is not critical. This implies that the end point $(\mu^*,0)$ is not multicritical but a simple critical point in the same universality class (viz., the PC class) as the generic transition at $\mu>\mu^*$. In fact, the end point can be understood as the critical point of the BARW2 domain-wall dynamics in the limit $\sigma\to 0$.

To test this hypothesis, we first study the survival probability and density of active sites as μ^* is approached along the μ axis. The inset of Fig. 8 shows the stationary survival probability (more precisely, its saturation value for $\sigma\to 0$) as a function of μ. The data can be well fitted by a power-law $P_s\sim(\mu^*-\mu)^{\beta}$ with $\beta=0.87(5)$. The corresponding information on the stationary density of active sites can be obtained from inset (b) of Fig. 7. It shows the prefactor B_μ of the linear σ-dependence $\rho_{st}=B_\mu\sigma$ as a function of $\mu^*-\mu$. Sufficiently close to μ^*, their relation can be fitted by a power law

$B_\mu \sim (\mu^* - \mu)^{\kappa^*}$ with $\kappa^* = 0.91$. Thus both β and κ^* agree with the order parameter exponent of the PC universality class within their error bars. This confirms the validity of the domain-wall theory of Sec. IV D at μ^*.

The discussion of the σ-dependence of P_s and ρ_{st} right at μ^* is somewhat more complicated because it is determined by the *subleading* σ-dependencies of the domain-wall rates Γ and Ω. Moreover, because the dynamics is extremely slow at $\mu \approx \mu^*$ and $\sigma \ll 1$, our numerical results close to the end point are less accurate then our other results. According to the domain-wall theory of Sec. IV D, the stationary survival probability should fulfill the homogeneity relation

$$P_s(\Delta\mu, \sigma) = b^{\beta/\nu^\perp} P_s(\Delta\mu b^{-1/\nu^\perp}, \sigma b^{-y^*}), \tag{12}$$

where $\Delta\mu = \mu - \mu^*$ while β and $\nu^\perp$ are the order parameter and correlation length exponents of the BARW2 transition (PC universality class). The only unknown exponent is y^*. The same homogeneity relation should hold for the domain-wall density, but *not* the density of active sites.

Setting the scale factor to $b = \sigma^{1/y^*}$ gives the scaling form

$$P_s(\Delta\mu, \sigma) = \sigma^{\beta/(\nu^\perp y^*)} Y(\Delta\mu \sigma^{-1/(\nu^\perp y^*)}). \tag{13}$$

Right at the end point, $\Delta\mu = 0$, this gives $P_s \sim \sigma^{\beta/(\nu^\perp y^*)}$. To test this power-law relation and to determine y^*, we performed spreading simulations at $\mu = \mu^*$ and several σ between 0.03 and 1. The low-σ behavior (not shown) can indeed be fitted by a power law in σ with an exponent $\beta/(\nu^\perp y^*) = 0.5(1)$. Using the well-known values $\beta = 0.92$ and $\nu^\perp = 1.83$ of the PC universality class, we conclude $y^* = 1.0(2)$. Within the domain-wall theory, $\rho_{DW} \sim P_s$ and the stationary density of active sites is $\rho_{st} \sim \sigma\rho_{DW} \sim \sigma^{\omega^*}$ with $\omega^* = 1 + \beta/(\nu^\perp y^*) = 1.5(1)$. This agrees well with the numerical estimate of 1.4(1) obtained from the density decay simulations in Fig. 7.

The scaling form [Eq. (13)] can also be used to determine the shape of the phase boundary at $\mu > \mu^*$. The phase boundary corresponds to a singularity of the scaling function Y at some nonzero value of its argument. Thus, the phase boundary follows the power law $\sigma \sim (\mu - \mu^*)^{\nu^\perp y^*}$. At fit of the data in Fig. 1 lead to $\nu^\perp y^* = 1.8(2)$ which implies $y^* = 1.0(1)$ in agreement with the above estimate from the spreading simulation data.

To investigate the time dependence of P_s close to the end point, the homogeneity relation (12) can be generalized to include a time argument. On the right hand side, it appears in the scaling combination $(t/t_0)b^z$ with t_0 the basic microscopic time scale. It is important to realize that this *microscopic* scale diverges as σ^{-1} with $\sigma \to 0$ (independent of any criticality at μ^*). Thus, the right scaling combination is actually $t\sigma b^z$. We used the resulting scaling theory to discuss the power-law decay of P_s on the phase boundary shown in Fig. 5(a). The scaling theory predicts $P_s \sim \sigma^{-\zeta} t^{-\delta}$ with $\zeta \equiv \delta$ as the end point is approached. This agrees with our numerical data [shown in the inset of Fig. 5(a)] which give $\zeta \approx 0.284$

In summary, all our simulation data support the notion that the end point $(\mu^*, 0)$ is a not a true multicritical point but a simple critical point in the same universality class (PC) as the entire generic phase boundary at $\mu \geq \mu^*$. The behavior of some observables makes it appear multicritical, though, because the microscopic time scale of the domain-wall dynamics diverges with $\sigma \to 0$.

V. CONCLUSIONS

In summary, we have studied the phase transitions of the generalized contact process with two absorbing states in one space dimension by means of large-scale Monte Carlo simulations. We have found that this model has two different nonequilibrium phase transitions, (i) the generic transition occurring for sufficiently high values $\mu > \mu^*$ of the healing rate and nonzero values of the boundary activation rate σ, and (ii) a transition at exactly $\sigma = 0$ for $\mu_c^{cp} < \mu < \mu^*$.

The generic transition is in the parity-conserving (PC) universality class (which coincides with the DP2 class in one dimension) everywhere on the $\mu \geq \mu^*$ phase boundary, in agreement with earlier work [13,17]. In contrast, the $\sigma = 0$ transition turned out to be *not* critical. The density of active sites rather goes to zero with the vanishing boundary activation rate σ while the survival probability remains finite for $\sigma \to 0$. Its behavior is controlled by the BARW2 dynamics of the domain walls between different inactive domains (which is not critical for $\mu_c^{cp} < \mu < \mu^*$). It is interesting to note that the behavior of our model at $\sigma \equiv 0$ differs qualitatively from the $\sigma \to 0$ limit of the finite-σ behavior in the entire parameter region $\mu_c^{cp} < \mu < \mu^*$.

As a result, the crossover between directed percolation (DP) critical behavior at $\sigma \equiv 0$ and parity conserving (PC) critical behavior for $\sigma > 0$ does not take the naively expected simple scaling form. In particular, the generic ($\sigma > 0$) phase boundary does not continuously connect to the critical point of the $\sigma \equiv 0$ theory (the simple contact process critical point). Instead, it terminates at a separate end point $(\mu^*, 0)$ on the μ-axis. While this point shares some characteristics with a multicritical point, it is actually just a simple critical point in the same universality class (PC) as the entire generic phase boundary.

We emphasize that the crossover between the DP and PC universality classes as a function of σ in our model is very different from that investigated by Odor and Menyhard [20]. These authors started from the PC universality class and introduced perturbations that destroy the symmetry between the absorbing states or destroy the parity conservation in branching and annihilating random walk models. They found more conventional behavior that can be described in terms of crossover scaling. In contrast, the transition rates (1) to (4) of our model do not break the symmetry between the two inactive states anywhere in parameter space.

Crossovers between various universality classes of absorbing state transitions have also been investigated by Park and Park [21–23]. They found a discontinuous jump in the phase boundary similar to ours along the so-called excitatory route from infinitely many absorbing states to a single absorbing state [21]. Moreover, there is some similarity between our mechanism and the so-called channel route [22] from the PC universality class to the DP class which involves an infinite number of absorbing states characterized by an

auxiliary density. In our case, at $\sigma \equiv 0$ (but not at any finite σ), any configuration consisting of I_1 and I_2 only can be considered absorbing because active sites cannot be created. The density of I_1-I_2 domain walls then plays the role of the auxiliary density; it vanishes at the end point $(\mu^*,0)$. However, our crossover occurs in the opposite direction than that of Ref. [22]: the small parameter σ takes the system from the DP universality class to the PC class. Note that an unexpected survival of active sites has also been observed in a version of the nonequilibrium kinetic Ising model with strong disorder. Here, the disorder can completely segment the system, and in odd-parity segments residual particles cannot decay [24].

The generalized contact process as defined in Eqs. (1)–(4) is characterized by *three* independent rates (one rate can be set to one by rescaling the time unit). In the bulk of our paper, we have focused on the case $\bar{\mu}=\mu$ for which our system reduces to the usual contact process in the limit of $\sigma \to 0$. In order to study how general our results are, we have performed a few simulation runs for $\bar{\mu} \neq \mu$ focusing on the fate of the end point that separates the generic transition from the $\sigma=0$ transition. The results of these runs are summarized in Fig. 9 which shows the phase diagram projected on the $\bar{\mu}-\mu$ plane. The figure shows that the line of end points of the generic phase boundary remains distinct from the simple contact process ($\sigma=0$) critical line in the entire $\bar{\mu}-\mu$ plane. The two lines only merge at the point $\bar{\mu}=0$, $\mu=1$ where the system behaves as compact directed percolation [13].

Our study was started because simulations at $\mu \gtrapprox \mu_c^{cp}$ and $\sigma \ll 1$ [18] seemed to suggest that the generalized contact process with two absorbing states is always active for any nonzero σ. The detailed work reported in this paper shows that this is *not* the case; a true inactive phase appears, but only at significantly higher $\mu > \mu^*$. Motivated by this result, we also carefully reinvestigated the generalized contact process with $n=3$ absorbing states which has been reported to be always active (for any nonzero σ) in the literature [13,17]. However, in contrast to the two-absorbing-states case, we could not find any inactive phase in this system.

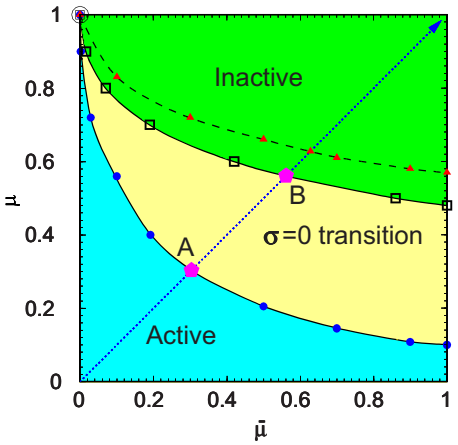

FIG. 9. (Color online) Projection of the phase diagram of the generalized contact process on the $\bar{\mu}-\mu$ plane. The individual symbols show the locations of the phase boundaries as determined from our simulations: solid blue circles—transition for $\sigma \equiv 0$ (simple contact process), solid red triangles—generic transition for $\sigma=1$, open squares—approximate location of the end point of the generic transition ($\sigma \to 0$) estimated from the transition at $\sigma=0.01$. The lines are guides to the eyes only. Points A and B are the simple contact process critical point and the end point investigated in the main part of the paper.

Let us close by posing the question of whether a similar splitting between the $n=1$ critical point and the $n=2$ phase transition line also occurs in *other* microscopic models with several absorbing states. Answering this questions remains a task for the future.

ACKNOWLEDGMENTS

We acknowledge helpful discussions with Geza Odor, Hyunggyu Park, and Ronald Dickman. This work has been supported in part by the NSF under Grant Nos. DMR-0339147 and DMR-0906566 as well as by Research Corporation.

[1] V. P. Zhdanov and B. Kasemo, Surf. Sci. Rep. **20**, 113 (1994).
[2] B. Schmittmann and R. K. P. Zia, in *Phase Transitions and Critical Phenomena*, edited by C. Domb and J. L. Lebowitz (Academic, New York, 1995), Vol. 17, p. 1.
[3] J. Marro and R. Dickman, *Nonequilibrium Phase Transitions in Lattice Models* (Cambridge University Press, Cambridge, England, 1999).
[4] H. Hinrichsen, Adv. Phys. **49**, 815 (2000).
[5] G. Odor, Rev. Mod. Phys. **76**, 663 (2004).
[6] S. Lübeck, Int. J. Mod. Phys. B **18**, 3977 (2004).
[7] U. C. Täuber, M. Howard, and B. P. Vollmayr-Lee, J. Phys. A **38**, R79 (2005).
[8] P. Grassberger and A. de la Torre, Ann. Phys. (N.Y.) **122**, 373 (1979).
[9] H. K. Janssen, Z. Phys. B **42**, 151 (1981).
[10] P. Grassberger, Z. Phys. B **47**, 365 (1982).
[11] P. Rupp, R. Richter, and I. Rehberg, Phys. Rev. E **67**, 036209 (2003).
[12] K. A. Takeuchi, M. Kuroda, H. Chate, and M. Sano, Phys. Rev. Lett. **99**, 234503 (2007).
[13] H. Hinrichsen, Phys. Rev. E **55**, 219 (1997).
[14] P. Grassberger, F. Krause, and T. von der Twer, J. Phys. A **17**, L105 (1984).
[15] D. Zhong and D. B. Avraham, Phys. Lett. A **209**, 333 (1995).
[16] T. E. Harris, Ann. Probab. **2**, 969 (1974).
[17] J. Hooyberghs, E. Carlon, and C. Vanderzande, Phys. Rev. E **64**, 036124 (2001).
[18] M. Y. Lee and T. Vojta, Phys. Rev. E **79**, 041112 (2009).
[19] I. Jensen, J. Phys. A **32**, 5233 (1999).
[20] G. Odor and N. Menyhard, Phys. Rev. E **78**, 041112 (2008).
[21] S.-C. Park and H. Park, Phys. Rev. E **76**, 051123 (2007).
[22] S.-C. Park and H. Park, Phys. Rev. E **78**, 041128 (2008).
[23] S.-C. Park and H. Park, Phys. Rev. E **79**, 051130 (2009).
[24] G. Odor and N. Menyhard, Phys. Rev. E **73**, 036130 (2006).